Journal of Statistical Physics, Vol. 101, No. 1/2, 2000

Modeling Thermostating, Entropy Currents, and Cross Effects by Dynamical Systems

Jürgen Vollmer,[1,2] **Tamás Tél,**[3] **and László Mátyás**[3]

Received March 22, 2000

A generalized multibaker map with periodic boundary conditions is shown to model boundary-driven transport, when the driving is applied by a "perturbation" of the dynamics localized in a macroscopically small region. In this case there are sustained density gradients in the steady state. A non-uniform stationary temperature profile can be maintained by incorporating a heat source into the dynamics, which deviates from the one of a bulk system only in a (macroscopically small) localized region such that a heat (or entropy) flux can enter an attached thermostat only in that region. For these settings the relation between the average phase-space contraction, the entropy flux to the thermostat and irreversible entropy production is clarified for stationary and non-stationary states. In addition, thermoelectric cross effects are described by a multibaker chain consisting of two parts with different transport properties, modeling a junction between two metals.

KEY WORDS: Deterministic chaos; spatial extension; multibaker maps; entropy balance; thermostating; thermoelectric cross effects.

1. INTRODUCTION

There is a recent interest in modeling transport processes by simple dynamical systems with chaotic dynamics. One class of models, actually inspired by Non-Equilibrium Molecular Dynamics (NEMD) simulations, describes systems driven by external fields with a spatially uniform dynamics subjected to periodic boundary conditions.$^{(1-7)}$ Another approach concentrates on systems driven from the boundaries, which lead to steady

---

[1] Fachbereich Physik, Univ.-GH Essen, 45117 Essen, Germany.

[2] Max Planck Institute for Polymer Research, Ackermannweg 10, 55128 Mainz, Germany.

[3] Institute for Theoretical Physics, Eötvös University, P.O. Box 32, H-1518 Budapest, Hungary.

states with sustained gradients of the thermodynamic fields.(8, 9) For a comparatively simple, but as far as their transport properties are concerned, generic class of dynamical systems, the *multibakers*,(10–20) we show that both mechanisms of driving can simultaneously be worked out. This leads to an improved understanding of the relation between the approaches. In the former approach transport is driven by a field acting uniformly in the full system, while in the latter case the driving is concentrated to a microscopic region in space. From this point of view, boundary-driven transport is closely analogous to transport in a dynamical system with periodic boundary conditions, which is driven out of equilibrium by a "perturbation" of the dynamics localized in a macroscopically small region.

In all models for transport, as emphasized by Nicolis and coworkers,(21, 22) a quantity of central interest is the heat flux, or equivalently the entropy flux, from the system into its environment. A central aim of modeling transport by dynamical systems is to identify settings, which are consistent with the thermodynamic entropy balance

$$\frac{dS}{dt} = \frac{d_e S}{dt} + \frac{d_i S}{dt} \tag{1}$$

i.e., with the statement that the temporal change of the thermodynamic entropy S can be decomposed into two contributions, called the external and internal change of the entropy, respectively. This integral form can be rewritten into a local balance equation when the two terms on the right hand side correspond to integrals of local densities. In that case, the time derivative of the entropy density s appears as

$$\partial_t s = \Phi + \sigma^{(irr)} \tag{2}$$

where Φ and $\sigma^{(irr)}$ represent the densities of the entropy flux and the rate of irreversible entropy production, respectively. In the bulk of typical macroscopic systems the entropy flux can be written as the divergence of the entropy current $j^{(s)}$,

$$\Phi = -\nabla j^{(s)} \tag{3}$$

reflecting the fact that heat ($Tj^{(s)}$ is directly related to the heat current) can only be taken out of the system at its boundaries.(23) On the other hand, this form has to be generalized at positions where there is a heat current flowing into an attached thermostat, and in cases where the entropy current is not differentiable, like for instance across interfaces between different materials. In those cases the entropy flux is not a full divergence, and it need not even be defined as a density. Rather the flux should then be written as

$$\Phi = -\nabla j^{(s)} + \Phi^{(th)} \tag{4}$$

where $j^{(s)}$ is the entropy current in the system, and $\Phi^{(th)}$ accounts for a direct flow of entropy into the surroundings, which acts then as a thermostat.

In the present paper, we shall put special emphasis on the role of the entropy flux $\Phi^{(th)}$, and on exploring under which conditions it can vanish. We find conditions on how to model the entropy balance for thermodynamic bulk systems, and for macroscopic systems subjected to thermostating by either a localized sink for the entropy or a spatially uniform coupling to a thermostat.

The role of the thermodynamic entropy of dynamical systems is played by the coarse-grained Gibbs entropy, whose usefulness in understanding irreversibility from the point of view of dynamical systems is by now thoroughly explained in the literature.(24–27, 12–20) (For stochastically perturbed dynamical systems where noise generates a kind of coarse graining, see refs. 21 and 22.) The bulk dynamics is represented by a multibaker model driving two fields, the density ϱ and the the kinetic energy per particle T, with a local source density q for the latter.(17, 18) A connection with macroscopic transport equations is aimed at in a suitable defined continuum limit (the *macroscopic limit*), where the field T will be interpreted as a temperature, based on the experience that this quantity is closely related to the average kinetic energy per particle.

We shall consider a sequence of periodic models of increasing complexity. Model I corresponds to a homogeneous isothermal system described by a thermostating algorithm. In this model no entropy current is defined—its entire entropy flux stems from a $\Phi^{(th)}$. By allowing a spatial resolution of the isothermal system (Model II), a non-vanishing $-\nabla j^{(s)}$ term appears in the transient behavior, but vanishes in the steady state, where $\Phi^{(th)}$ remains unchanged. It is the only contribution to the flux in a steady state. Model III is still isothermal but with a locally deviating dynamics in one of the multibaker cells representing a boundary. The bulk dynamics can then be chosen so that (3) holds in the bulk, and all the heat taken out is concentrated in the boundary with a $\Phi^{(th)} \neq 0$ there. In model IV we allow for temperature changes and local heat sources. By taking q locally deviating from that of the bulk in one cell, we find a steady temperature profile with a bend (i.e., a jump in its first derivative) at the boundary. The q distribution can then be chosen such that again (3) holds in the bulk. The heat source in the boundary is however singular.

It corresponds exactly to the one which follows from thermodynamics. Finally, we consider a multibaker chain joined together from two subchains with different material properties. This models a junction between two metals so that one can observe thermodynamic cross effects, like the Peltier and Seebeck effects, very much in the same arrangements as in classical experiments.

This paper is organized as follows. In Section 2 the local dynamics of the considered multibaker model is defined, and its local entropy balance is worked out. In Section 3, Model I–Model IV are treated, which share periodic boundary conditions and represent thermodynamic settings of increasing complexity. Section 4 is devoted to cross-effects. We conclude with a short discussion in Section 5.

2. LOCAL TRANSPORT AND THERMODYNAMIC RELATIONS FOR MULTIBAKERS

In this section we describe the local dynamics of a cell of a multibaker map modeling a system with particle(20, 12–16) and heat transport.(17, 18) We work out its density and kinetic-energy dynamics, and present general relations for the entropy changes. The effect of boundary conditions will be considered in subsequent sections for a few models with progressively richer thermodynamics.

2.1. Phase-Space Dynamics of Multibaker Maps

The phase space (x, p) of the multibaker map consists of cells labeled by the index m (Fig. 1). The division of the x axis into cells corresponds to a partitioning of the configuration space into regions, sufficiently large to characterize the state inside the cell by thermodynamic variables and small enough to neglect variation of these variables on the length scale of the cells (*local equilibrium approximation*). Every cell has a width a and height $b \equiv 1$. The coordinates of individual particles in the cell are given as a position variable x, and a momentum-like variable p. We are interested in the dynamics of two dimensionless fields, the phase-space density $\varrho(x, p)$, and a field $T(x, p)$ characterizing the local kinetic energy per particle. After each time unit τ, every cell is divided into three columns (Fig. 1) with respective widths al_m, as_m and ar_m. (Note that $l_m + s_m + r_m = 1$ for every m.) The right (left) column of width ar_m (al_m) is uniformly squeezed and stretched into a strip of width a and of height l_{m+1} (r_{m-1}), which is mapped to the right (left) neighboring cell. The middle one preserves its area and remains in cell m. Note that the map is one-to-one on its domain. It globally preserves the phase-space volume, but it can *nevertheless* locally

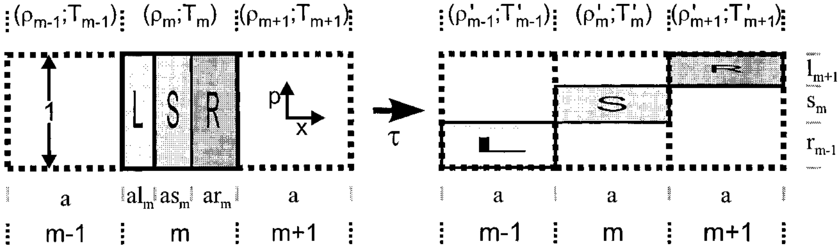

Fig. 1. Graphical illustration of the action of the multibaker map on cell m. The letters L, S and R are inserted to visualize this action. Iteration of the rule after every time unit τ defines the time evolution. More details about the action of the mapping and the symbols needed for its definitions are given in the text. The symbols ϱ_i and T_i indicated on the margins show the average values of the fields on the cells and on its neighbors ($i = m; m \pm 1$).

expand or contract the phase-space volume. In refs. 14 and 18 it was argued that only the choice of the contraction factors given here can be consistent with thermodynamics (one can find an analogous formulation with a fully area preserving dynamics at the expense of a spatial variation of the volume of the cells of the multibaker; cf. ref. 19).

The field T is advected by the particle dynamics, and—in order to mimic a local heating of the system—it is also multiplied by a factor $(1 + \tau q)$ depending on the averages characterizing the local currents and the thermodynamic state. By this a *mean-field-like* coupling of the motion of the particles in and around of a given cell is introduced. The source term q will appear in the equation describing the time-evolution of the kinetic energy density, where it expresses that the kinetic energy is not a conserved quantity. Furthermore, it will characterize the entropy flux into the thermostat. By choosing different functional forms of q, different couplings to the thermostat can be described (cf. Subsection 2.5).

In general, the width al_m, as_m, and ar_m of the columns may depend on the variables characterizing the thermodynamic state in the vicinity of the cell, so that they vary in time and space. This is indicated by the explicit dependence of the parameters on the cell index m.

Iteration of these rules defines the time evolution of the system. The (x, p) dynamics generates ever refining structures in the distributions $\varrho(x, p)$ and $T(x, p)$. For simplicity, we take the fields initially constant in each cell: $\varrho(x, p) = \varrho_m$, $T(x, p) = T_m$. After one step of iteration, the fields will be piecewise constant on the strips defined in Fig. 1. Due to the conservation of particles, the phase-space density in cell m takes the respective values

$$\varrho'_{m,r} = \frac{r_{m-1}}{l_m} \varrho_{m-1}, \qquad \varrho'_{m,s} = \varrho_m, \qquad \varrho'_{m,l} = \frac{l_{m+1}}{r_m} \varrho_{m+1} \tag{5}$$

(The prime will always indicate quantities evaluated after one time step.) The contraction factors l_m/r_{m-1} and r_m/l_{m+1} are the Jacobians corresponding to the mapping from cell $m-1$ to m and from cell $m+1$ to m, respectively. After division by τ the logarithm of the factors gives the negative of the local phase-space contraction rates. We define the phase-space contraction rate σ_m of cell m as the the weighted average of these two local contributions:

$$\sigma_m = \frac{1}{\tau}\left[\varrho_{m-1} r_{m-1} \ln \frac{r_{m-1}}{l_m} + \varrho_{m+1} l_{m+1} \ln \frac{l_{m+1}}{r_m}\right] \tag{6}$$

The Jacobian corresponding to the dynamics of the central region (S) is unity so it does not contribute to σ_m.

2.2. Dynamics of the Particle Density and the Particle Current

After one time step, the average density ϱ'_m in cell m is a weighted average of $\varrho'_{m,r}$, $\varrho'_{m,s}$, and $\varrho'_{m,l}$. It is determined by its initial density ϱ_m and by the initial densities $\varrho_{m\pm 1}$ of the neighboring cells. Multiplying the strip densities (2.1) with the widths of the respective strips, adding them up and dividing the sum by the width a of the cell, one obtains the average (or the *coarse-grained*) density after the iteration

$$\varrho'_m = s_m \varrho_m + r_{m-1} \varrho_{m-1} + l_{m+1} \varrho_{m+1} \tag{7}$$

The coarse-grained density evolves according to this master equation, which can be rearranged to obtain the discrete conservation law of the density

$$\frac{\varrho'_m - \varrho_m}{\tau} = -\frac{j_m - j_{m-1}}{a} \tag{8}$$

Here

$$j_m = \frac{a}{\tau}\left(r_m \varrho_m - l_{m+1} \varrho_{m+1}\right) \tag{9}$$

is the discrete particle current through the right boundary of cell m.

2.3. The Kinetic-Energy Dynamics and the Energy Current

According to the T dynamics described above the updated values $T'_{m,r}$, $T'_{m,s}$, $T'_{m,l}$ for T on the respective strips R, S, L of cell m contain a source term characterized by a local strength q_m:

$$\begin{aligned} T'_{m,r} &= T_{m-1}[1+\tau q_m] \\ T'_{m,s} &= T_m[1+\tau q_m] \\ T'_{m,l} &= T_{m+1}[1+\tau q_m] \end{aligned} \tag{10}$$

This strength is yet undetermined. It depends on the physical setting of thermostating to be modeled and on the average of ϱ and T values in the cells and in its neighbors.

The (x, p) dynamics also drives the field ϱT. After one iteration the kinetic-energy density of cell m takes the value

$$\varrho'_m T'_m = [s_m \varrho_m T_m + r_{m-1} \varrho_{m-1} T_{m-1} + l_{m+1} \varrho_{m+1} T_{m+1}](1+\tau q_m) \tag{11}$$

This equation can be rearranged as a discrete balance equation for the time evolution of ϱT:

$$\frac{\varrho'_m T'_m - \varrho_m T_m}{\tau} = \varrho'_m T'_m \frac{q_m}{1+\tau q_m} - \frac{j_m^{(\varrho T)} - j_{m-1}^{(\varrho T)}}{a} \tag{12}$$

where $j_m^{(\varrho T)} = T_m j_m - (a^2 l_{m+1}/\tau)\, \varrho_{m+1}(T_{m+1} - T_m)/a$ is a corresponding discrete energy current. Note that the r.h.s of (12) is not a full divergence, in accordance with the fact that the kinetic energy is not a conserved quantity. In an isothermal system where there is no kinetic energy dynamics, no source can be present ($q_m = 0$).

2.4. Gibbs Entropy and the Coarse-Grained Entropy

In this study we are interested in both the temporal evolution of the exact fields $\varrho(x, p)$ and $T(x, p)$, and in the evolution of their respective cell averages ϱ_m and T_m. The former characterize the microscopic time evolution, while the averages describe the local thermodynamic state in spatially small regions. Both levels of description admit entropy functionals, which are commonly denoted as Gibbs and coarse-grained entropies.

The Gibbs entropy $S^{(G)}$ is related to the detailed knowledge of the system. It is taken with respect to the exact densities $\varrho(x, p)$ and $T(x, p)$. In a given cell it is defined as

$$S_m^{(G)} = -\int_{\text{cell } m} dx\, dp\, \varrho(x, p) \ln\left(\frac{\varrho(x, p)}{\varrho^\star} T(x, p)^{-\gamma}\right) \tag{13}$$

Here, $\varrho^\star T^\gamma$ plays the role of a local T-dependent reference density with a constant reference density $\varrho^\star$ and γ as a yet undetermined constant. In ref. 18 it is demonstrated that only this choice of the T-dependent reference density can be consistent with thermodynamics.

The coarse-grained entropy S_m has a similar form, but it is based on the averaged values in the considered cell:

$$S_m = -a\varrho_m \ln\left(\frac{\varrho_m}{\varrho^\star} T_m^{-\gamma}\right) \tag{14}$$

The reference density $\varrho^\star$ in the expression of the coarse-grained entropy coincides with the one chosen for the Gibbs entropy.

As mentioned above, throughout the paper we only consider initial distributions, which are uniform in every cell (cf. refs. 14, 16, and 18 for more general choices). As a consequence, initially $S_m = S_m^{(G)}$, and after one time step the entropies become

$$\begin{aligned} S_m^{(G)\prime} = -a\Bigg[& s_m\varrho_m \ln\left(\frac{\varrho_m}{\varrho^\star} T'^{-\gamma}_{m,s}\right) + r_{m-1}\varrho_{m-1} \ln\left(\frac{\varrho'_{m,r}}{\varrho^\star} T'^{-\gamma}_{m,r}\right) \\ & + l_{m+1}\varrho_{m+1} \ln\left(\frac{\varrho'_{m,l}}{\varrho^\star} T'^{-\gamma}_{m,l}\right)\Bigg] \end{aligned} \tag{15}$$

and

$$S'_m = -a\varrho'_m \ln\left(\frac{\varrho'_m}{\varrho^\star} T'^{-\gamma}_m\right) \tag{16}$$

2.5. Entropy Balance

The coarse-grained entropy fulfills a local entropy balance in direct analogy to the one in irreversible thermodynamics. To derive this equation one identifies at any given time the difference $S_m - S_m^{(G)}$ as the information on the microscopic state of the system which cannot be resolved in the coarse-grained description. The temporal change of this lack of information is then identified with the irreversible entropy production $\Delta_i S_m$, and the change $(S'^{(G)}_m - S_m^{(G)})$ of the Gibbs entropy with the entropy flux $\Delta_e S_m$. Thus,

$$\frac{S'_m - S_m}{\tau} = \frac{\Delta_e S_m}{\tau} + \frac{\Delta_i S_m}{\tau} \tag{17}$$

which is a discrete analog of (1).

The form of the entropy production is [cf. (15) and (16)]:

$$\frac{\Delta_i S_m}{\tau}=\frac{[S'_m-S_m^{(G)\prime}]-[S_m-S_m^{(G)}]}{\tau}$$
$$=\frac{a}{\tau}\left[-\varrho'_m\ln\left(\frac{\varrho'_m T'^{\,-\gamma}_m}{\varrho_m T'^{\,-\gamma}_{m,s}}\right)+\varrho_{m-1}r_{m-1}\ln\left(\frac{\varrho'_{m,r}T'^{\,-\gamma}_{m,r}}{\varrho_m T'^{\,-\gamma}_{m,s}}\right)\right.$$
$$\left.+\varrho_{m+1}l_{m+1}\ln\left(\frac{\varrho'_{m,l}T'^{\,-\gamma}_{m,l}}{\varrho_m T'^{\,-\gamma}_{m,s}}\right)\right] \tag{18}$$

where we used that $S_m-S_m^{(G)}$ vanishes due to the particular choice of initial conditions.

The entropy flux becomes

$$\frac{\Delta_e S_m}{\tau}=-\frac{a}{\tau}\left[(\varrho'_m-\varrho_m)\ln\left(\frac{\varrho_m}{\varrho^\star}T_m^{-\gamma}\right)+\varrho'_m\ln\frac{T'^{\,-\gamma}_{m,s}}{T_m^{-\gamma}}\right.$$
$$\left.+\varrho_{m-1}r_{m-1}\ln\left(\frac{\varrho'_{m,r}}{\varrho_m}\frac{T'^{\,-\gamma}_{m,r}}{T'^{\,-\gamma}_{m,s}}\right)+\varrho_{m+1}l_{m+1}\ln\left(\frac{\varrho'_{m,l}}{\varrho_m}\frac{T'^{\,-\gamma}_{m,l}}{T'^{\,-\gamma}_{m,s}}\right)\right] \tag{19}$$

which can be split into a divergence of an entropy current and a flux into the thermostat

$$\frac{\Delta_e S_m}{a\tau}=-\frac{j_m^{(s)}-j_{m-1}^{(s)}}{a}+\Phi_m^{(th)} \tag{20}$$

with

$$j_m^{(s)}\equiv -j_m\ln\left(\frac{\varrho_m}{\varrho^\star}T_m^{-\gamma}\right)+\frac{a l_{m+1}}{\tau}\varrho_{m+1}\ln\left(\frac{\varrho_{m+1}}{\varrho_m}\frac{T_{m+1}^{-\gamma}}{T_m^{-\gamma}}\right)-\frac{a}{\tau}(r_m-l_m)\,\varrho_m \tag{21a}$$

$$\Phi_m^{(th)}\equiv -\frac{1}{\tau}\left[\varrho'_m\ln\frac{T'^{\,-\gamma}_{m,s}}{T_m^{-\gamma}}+r_{m-1}\varrho_{m-1}\ln\left(\frac{r_{m-1}}{l_m}\frac{T'^{\,-\gamma}_{m,r}T_m^{-\gamma}}{T'^{\,-\gamma}_{m,s}T_{m-1}^{-\gamma}}\right)\right.$$
$$\left.+l_{m+1}\varrho_{m+1}\ln\left(\frac{l_{m+1}}{r_m}\frac{T'^{\,-\gamma}_{m,l}T_m^{-\gamma}}{T'^{\,-\gamma}_{m,s}T_{m+1}^{-\gamma}}\right)\right]$$
$$-\frac{(r_m-l_m)\,\varrho_m-(r_{m-1}-l_{m-1})\,\varrho_{m-1}}{\tau} \tag{21b}$$

Note that (20) is a discrete counterpart of (4), and $j_m^{(s)}$ and $\Phi_m^{(th)}$ are the discrete entropy current and entropy flux to the thermostat, respectively.

2.6. The Macroscopic Limit

The projection of the multibaker dynamics on the x axis corresponds to a biased random walk with some diffusion coefficient and drift. The drift has to be present if we want to model non-equilibrium systems subjected to electric fields and/or temperature gradients. The requirement of consistency with an advection diffusion equation in the large system and long time limit, when the cell size is much smaller than the system size, and the time unit is much shorter than the macroscopic relaxation time, leads(12, 14, 15, 18) to the scaling relation:

$$r_m = \frac{\tau D}{a^2}\left(1 + \frac{a v_m}{2D}\right) \tag{22a}$$

$$l_m = \frac{\tau D}{a^2}\left(1 - \frac{a v_m}{2D}\right) \tag{22b}$$

We allow for a location dependence of the drift v_m but assume that the diffusion coefficient D is spatially constant. The continuum limit of the multibaker dynamics, which is taken with these constraints, is called the *macroscopic limit*. Formally, it corresponds to taking $a, \tau \to 0$ while keeping D fixed, and a, ϱ_m, T_m, v_m and q_m finite so that they approach a macroscopic position coordinate x, and smooth functions $\varrho(x)$, $T(x)$, $v(x)$ and $q(x)$, respectively. After taking this limit we call $\varrho(x)$ the density and $T(x)$ the temperature distribution in the system. The macroscopic limit of all the local relations given in (7)–(19) can be worked out explicitly.(12, 14, 15, 17) In the following this limit will be indicated by an arrow "→." Here we only mention that the system's equation of state turns out(17, 18) to be that of a classical ideal gas with $\gamma\varrho$ as its heat capacity (measured in units of Boltzmann's constant).

3. PERIODIC MODELS

3.1. Model I: Isothermal Single-Cell Multibaker for Field Driven Transport

We start by discussing the simplest conceivable model for describing a macroscopic transport process. A particle current induced by an external field in an isothermal environment described by a single baker cell subjected to periodic boundary conditions. The right boundary of the cell is identified with its left boundary and the mapping is from the cell onto itself. Because of driving $r \neq l$, and thermostating is applied via the appearance of the contraction factors l/r and r/l in order to reach a steady state. This mapping

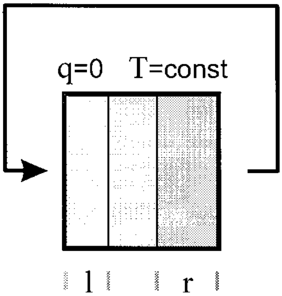

Fig. 2. Isothermal single-cell periodic baker map. The right boundary is identified with the left one. In this and all following figures the indicated width of the strips (i.e., l, r) is to be understood as the fraction of the total width of a of the cell.

propagates the coordinates of a large number of particles, which do not interact, i.e., they all are mapped by the same mapping. Clearly, this system does not admit a spatial resolution of the densities characterizing the transport process. Its local and global behavior coincides, so that the subscript m of the densities can be discarded in this case.

For the single-cell multibaker the master equation (7) predicts $\varrho' = \varrho \equiv \bar{\varrho}$. This implies that the model describes transport in a steady state with the average density $\bar{\varrho}$. The particle current $j = (a/\tau)(r - l)\, \bar{\varrho} = v\bar{\varrho}$ is constant in space and time, and the entropy production (18) becomes ($T = \text{const}$)

$$\frac{\Delta_i S}{a\tau} = \bar{\varrho}\, \frac{(r-l)}{\tau} \ln\left(\frac{r}{l}\right) \equiv \sigma \tag{23}$$

It has the macroscopic limit:

$$\frac{\Delta_i S}{a\tau} \to \sigma^{(irr)} = \bar{\varrho}\, \frac{v^2}{D} \tag{24}$$

In a similar way, the entropy flux (20), (21b) has the macroscopic form

$$\frac{\Delta_e S}{a\tau} \to \Phi^{(th)} = -\bar{\varrho}\, \frac{v^2}{D} \tag{25}$$

As expected in a steady state, $\Delta_i S$ and $\Delta_e S$ add up to zero. More interestingly, however, these contributions to the change of entropy are also directly proportional to the local phase-space contraction (6), which reduces to $\bar{\varrho} v^2/D$ in the macroscopic limit.

3.2. Model II: Isothermal Multibaker Chain for Field Driven Transport

In the single-cell multibaker the coarse-grained density cannot evolve in time, since no spatial variations are resolved. For this reason, one also cannot distinguish between the local entropy balance as described by (2), (4) and the balance (1) for the full macroscopic system. In order to address these points, we generalize the previous setting by considering a multibaker chain of $N+1$ cells, with spatially constant driving (i.e., $r_m = r$ and $l_m = l$) and periodic boundary conditions: cell $N+1$ and cell 0 are identified. From (9) we obtain for the particle current

$$j_m = \frac{a}{\tau}\left[(r-l)\,\varrho_m - l(\varrho_{m+1} - \varrho_m)\right] \tag{26}$$

which has the macroscopic limit:

$$j_m \to j \equiv \varrho v - D\partial_x \varrho \tag{27}$$

This current varies along the chain as long as the cell densities evolve in time. The asymptotic state, however, is formed by a spatially uniform density distribution with the average density $\bar{\varrho}$.

For constant temperature T the irreversible entropy production (18) becomes

$$\frac{\Delta_i S_m}{a\tau} = \frac{1}{\tau}\left[-\varrho'_m \ln\frac{\varrho'_m}{\varrho_m} + r\varrho_{m-1}\ln\left(\frac{\varrho_{m-1}}{\varrho_m}\frac{r}{l}\right) + l\varrho_{m+1}\ln\left(\frac{\varrho_{m+1}}{\varrho_m}\frac{l}{r}\right)\right] \tag{28}$$

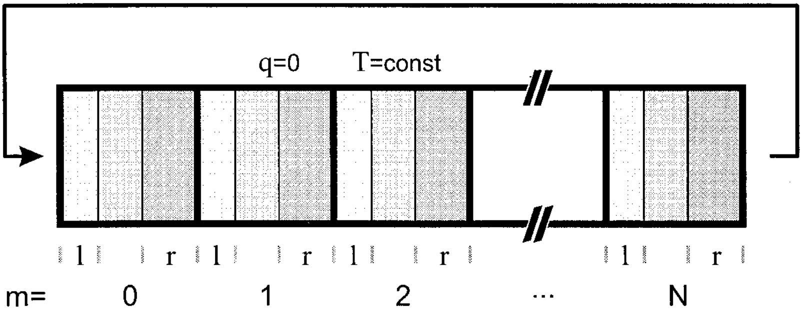

Fig. 3. Isothermal multibaker chain of $N+1$ cells. The right boundary of cell N is identified with the left boundary of cell 0.

Using (7) and (22), a lengthy but straightforward calculation$^{(14)}$ shows that in the macroscopic limit $a, \tau \to 0$ and $aN = \text{const}$ this *local* form is consistent with thermodynamics since in a general non-steady state it approaches

$$\sigma^{(irr)} = \frac{(\varrho v - D\partial_x \varrho)^2}{\varrho D} = \frac{j^2}{\varrho D} \tag{29}$$

In a similar way,$^{(14, 15)}$ the entropy flux (19) can be calculated, which in the macroscopic limit has the form (4), with the entropy current

$$j^{(s)} = -j\left[1 + \ln\left(\frac{\varrho}{\varrho^{\star}}\right)\right] \tag{30}$$

and the entropy flux

$$\Phi^{(th)} = -\frac{vj}{D} \tag{31}$$

transferred directly to the environment. This local expression expresses that every cell is coupled to the thermostat. In the steady state the coarse-grained density is constant along the chain $\varrho = \bar{\varrho}$ and the current takes the form $j = \bar{\varrho} v$, such that $\partial_x j^{(s)}$ vanishes, and we recover (24) and (25).

Due to the additional spatial resolution (as compared to Model I) the local and global features of the entropy balance can be different. It is worth considering the global entropy production, defined as [cf. (28)]

$$\sum_{m=0}^{N} \frac{\varDelta_i S_m}{\tau} = \frac{a}{\tau}\left[\sum_{m=0}^{N} \varrho_m\right](r-l)\ln\left(\frac{r}{l}\right) + \frac{a}{\tau}\sum_{m=0}^{N}\left[-\varrho'_m \ln \varrho'_m + \varrho_m \ln \varrho_m\right] \tag{32}$$

Here, the logarithms of ratios of densities of neighboring cells in (28) drop out in the sum due to the periodic boundary conditions. The global entropy production takes then the macroscopic form

$$\sum_{m=0}^{N} \frac{\varDelta_i S_m}{\tau} \to \frac{d_i S}{dt} = \left[\sum_{m=0}^{N} a\varrho_m\right]\frac{v^2}{D} - \sum_{m=0}^{N} a\partial_t[\varrho \ln \varrho] = \mathcal{N}\frac{v^2}{D} + \frac{dS}{dt} \tag{33}$$

where $\mathcal{N} = a\bar{\varrho}(N+1)$ is the total number of particles in the multibaker chain, and $S = \sum_m S_m$ is the total entropy.

The global form of the entropy flux is [cf. (19)]

$$\sum_{m=0}^{N} \frac{\varDelta_e S_m}{\tau} = -\frac{a}{\tau}\left[\sum_{m=0}^{N} \varrho_m\right](r-l)\ln\left(\frac{r}{l}\right) = -\sum_{m=0}^{N} a\sigma_m \tag{34}$$

which takes the macroscopic limit

$$\sum_m \frac{\Delta_e S_m}{\tau} \to \frac{d_e S}{dt} = -\mathcal{N} \frac{v^2}{D} \tag{35}$$

This shows that the local and the global entropy balances are markedly different. Locally, the entropy current depends only on the local current and the local density. There is only an indirect influence of the drift velocity v through its contribution to the current and its influence on the density profile. In contrast, the macroscopic flux only depends on the total number of particles in the system and on the drift velocity. It is constant in time since it neither depends on the current nor on the density profile, which in general both evolve in time. Interestingly, also in this more general setting the negative of the global entropy flux equals the (total) phase-space contraction rate at any time. This is in full harmony with the result obtained for the entropy flux in noisy dynamical systems by Nicolis and Daems.(21, 22) In contrast, the total irreversible entropy production is in general no longer directly related to the phase-space contraction. Its local form exactly amounts to Joule's heating $j^2/\varrho D$, and globally it picks up an additional contribution characterizing the time-evolution of the macroscopic states. Therefore, the often cited relation(1, 3, 5, 24, 28) between the global entropy production and the phase-space contraction only holds in steady states, where the modulus of the entropy flux coincides with the rate of entropy production.

3.3. Model III: Isothermal Multibaker Chain with Driving Localized to a Single Cell

A generalization of the previous case is a system modeling boundary-driven transport. Here, we consider a setting with periodic boundary conditions. Away from the point of driving, the steady-state macroscopic properties correspond to those of boundary-driven transport, but due to the periodic boundary condition the model is a well-defined dynamical system, which sheds new light on our previous models.(14, 15)

We consider a multibaker chain where cell 0 has a behavior different from the rest of the chain in the sense that its drift velocity differs from that of the bulk where $r = l$ (i.e., $v = 0$). The diffusion coefficient, however, is still the same in all cells. This implies $r_0 - r = l - l_0 \neq 0$ [cf. (22)]. The driving in cell zero has the tendency to generate an accumulation of particles right, and a

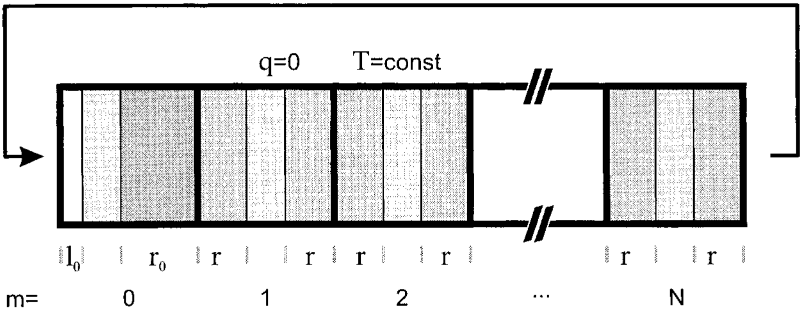

Fig. 4. Isothermal multibaker chain with driving in cell 0. There is no drift in the bulk.

slowly decreasing density distribution on its left (we assume $v_0 > 0$, $r_0 > r$). In a steady state, this leads to a linear density profile

$$\varrho_m = \bar{\varrho} + \left(\frac{N-1}{2} - m + 1 \right) \delta\varrho \qquad \text{for} \quad m = 1, \ldots, N \tag{36}$$

whose increment $\delta\varrho$ is uniquely determined by r_0 (or v_0). In cell zero we find $\varrho_0 = \bar{\varrho}$. A substitution into the master equation for $m = 1$ or N leads to

$$\delta\varrho = \bar{\varrho} \frac{2}{N+1} \left(\frac{r_0}{r} - 1 \right) \tag{37}$$

Again the average density $\bar{\varrho}$ is related to the number of particles $\mathcal{N}$ in the system via $a\bar{\varrho}(N+1) = \mathcal{N}$. By taking into account that according to (22) $r_0 = r[1 + av_0/(2D)]$, we obtain that $\delta\varrho$ is indeed proportional to v_0:

$$v_0 = D \frac{\delta\varrho}{a} \frac{N+1}{\bar{\varrho}} = D \frac{\delta\varrho}{a} \frac{\mathcal{N}}{a\bar{\varrho}^2} \tag{38}$$

The steady-state current is:

$$j = \bar{\varrho} \frac{v_0}{2} - D \frac{\varrho_1 - \bar{\varrho}}{a} = D \frac{\delta\varrho}{a} = \frac{v_0 \bar{\varrho}}{N+1} \tag{39}$$

The diffusion current of cells N and 0 is much stronger than otherwise, due to the sudden jump in the densities, but in the steady state the surplus is exactly compensated by the local drift currents. Thus the particle transport in the steady states of Model II and Model III are equivalent provided the drift v in the former coincides with $D\delta\varrho/(a\bar{\varrho})$ in the latter. As far as the steady-state transport is concerned, it does not matter, whether one applies a small uniform field leading to a spatially uniform drift v or a large one $v_0 = (N+1)\, v$ in a single cell only.

All thermodynamic relations of relevance can be worked out not only for the steady state (36), but for general non-steady states. The local forms of the entropy production and the entropy flux in the bulk are special cases of (29)–(31). Since $r = l$ in the bulk, there is no entropy flux into the thermostat $\Phi^{(th)} = 0$ for $m = 2,..., N-1$. On the other hand, the entropy flux in cell 0 and its neighbors does contain a part which cannot be written as a divergence. Due to (21b), the flux into the thermostat turns out to be:

$$\begin{aligned}\Phi^{(th)} \equiv \Phi_N^{(th)} + \Phi_0^{(th)} + \Phi_1^{(th)} &= \frac{1}{\tau}\left[(r\varrho_1 - r_0\varrho_0) \ln\left(\frac{r_0}{r}\right) - (r\varrho_N - l_0\varrho_0) \ln\left(\frac{r}{l_0}\right)\right] \\ &= -a(\sigma_N + \sigma_0 + \sigma_1) \end{aligned} \tag{40}$$

Again $\Phi^{(th)}$ is the negative of the total phase-space contraction rate:

$$\sum_{m=0}^{N} \frac{\Delta_e S_m}{\tau} = -\sum_{m=0}^{N} a\sigma_m \tag{41}$$

Assuming that $av_0 \ll 2D$

$$\Phi^{(th)} \approx \frac{v_0}{2} \frac{\varrho_1 - \varrho_N}{a} - \varrho_0 \frac{v_0^2}{4D} - \frac{\varrho_1 + \varrho_N}{2} \frac{v_0^2}{4D} \tag{42}$$

In the steady state $\varrho_N - \varrho_1 = -(N-1)\, \delta\varrho = -(N-1)\, aj/D$, $\varrho_0 = (\varrho_1 + \varrho_N)/2 = \bar{\varrho}$, and thus

$$\Phi^{(th)} \equiv -\frac{v_0 j}{D} \tag{43}$$

In the macroscopic limit the quantity $\delta\varrho/a$ approaches the gradient $-\partial_x \varrho$ in the bulk, $\bar{\varrho}$ and $\mathcal{N}$ stay constant and thus v_0 in (38) is proportional to $1/a$. The driving is singularly strong and so is the entropy flux density into the thermostat. By integrating, however, over the volume of cell zero and its neighbors we obtain the total entropy flux into the thermostat $-av_0 j/D = -j^2 \mathcal{N}/\bar{\varrho}^2 D$. It coincides with the macroscopic limit of the total entropy flux $\sum_{m=0}^{N} \Delta_e S_m/\tau$ since the integral of $\partial_x j^{(s)}$ vanishes in a periodic system, i.e.,

$$\frac{d_e S}{dt} = -\frac{j^2}{\bar{\varrho} D} \frac{\mathcal{N}}{\bar{\varrho}} \tag{44}$$

This result is equivalent to the steady-state version of (35) expressed by the current.

In this model there is no need for taking out entropy (heat) along the bulk. Thermostating is active in cell 0 and its neighbors only. It extracts exactly the same entropy flux there as the full entropy flux of Model II in the steady state. Thus the models refer to two different realizations of thermostating the transport process.(8) Model II should be viewed as, e.g., a wire which is kept at constant temperature by removing the heat due to dissipation everywhere along its length—Model III is closer related to a thermally isolated system, where heat is transported to the "boundary," from where the system is driven. For the multibaker this takes place in the special cell $m = 0$. Boundary driven transport typically leads, however, to non-uniform temperature profiles. A full treatment of such transport processes should be based therefore on a multibaker chain with kinetic-energy dynamics.

3.4. Model IV: Multibaker Chain with Thermostating Localized to a Single Cell

In the realm of classical thermodynamics heat is transported to the boundaries of the system. If, however, there is a bend in the temperature profile, a jump in the heat current occurs and heat is taken out at this point.

In order to model such a situation, we consider a multibaker chain with kinetic-energy dynamics and with fixed transition probabilities ($r_m = r$, $l_m = l$, $m = 0, 1,..., N$). The general relation (18) and a calculation similar to the one leading to (29) yields in the macroscopic limit for the entropy production(18)

$$\sigma^{(irr)} = \lambda \left(\frac{\partial_x T}{T} \right)^2 + \frac{j^2}{\varrho D} \tag{45}$$

Here, $j = \varrho v - D \partial_x \varrho$ is the particle current, and $\lambda = \gamma \varrho D$ is the heat conductivity of the model. From (19)–(21) we obtain

$$\Phi^{(th)} = \gamma \varrho q - \frac{vj}{D} \tag{46}$$

as the entropy flux let directly into the thermostat, and

$$j^{(s)} = -\lambda \frac{\partial_x T}{T} + \frac{e\Pi}{T} j \tag{47}$$

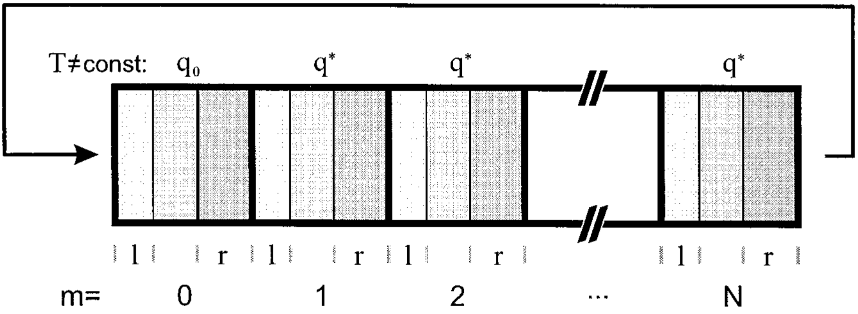

Fig. 5. Non-isothermal multibaker chain with thermostating localized to cell 0. The local heat source q_0 of that cell is different from that in the bulk, which is $q^* = -vj/D$.

as the entropy current where Π is the bulk Peltier coefficient

$$\frac{e\Pi}{T} = -\left(1 + \ln\frac{\varrho T^{-\gamma}}{\varrho^\star}\right) \tag{48}$$

and e represents the charge of the particles. Note that there is always a possibility to "close" the system locally in the sense that the source term $q = q^\star = vj/\lambda$ is chosen such that $\Phi^{(th)}$ vanishes.

We consider a periodic chain with fixed transition probabilities. The local heating sources take the value $q_m = q^\star$ in the bulk $m = 1, ..., N$, but there is a different source q_0 in cell 0. In the steady state we find a constant particle density along the chain. Inside the bulk, the kinetic-energy equation (11) implies for the steady temperature distribution

$$T_m = [(1-r-l)\,T_m + rT_{m-1} + lT_{m+1}](1+\tau q^*) \tag{49}$$

With periodic boundary conditions ($T_{m=0} = T_0$, and $T_{m=N+1} = T_0$) this equation has the general solution

$$T_m = \frac{T_0}{\sin[b(N+1)]}\left(\frac{r}{l}\right)^{m/2}\left\{\sin[b(N+1)-bm] + \left(\frac{l}{r}\right)^{(N+1)/2}\sin(bm)\right\} \tag{50}$$

where

$$\cos b = \sqrt{rl}\left(1 - \frac{\tau q^\star}{(1+\tau q^\star)(r+l)}\right) \tag{51}$$

The solution (50) has a bend in cell zero, in the sense that the left and right derivatives are different. Only at this location in the system the entropy flux is not a full divergence. Applying the kinetic-energy equation (11) to cell zero in a steady state, where the density is constant, we find that

$$q_0 = \frac{1}{\tau} \frac{r(T_0 - T_N) + l(T_0 - T_1)}{(1 - r - l)\ T_0 + rT_N + lT_1} \tag{52}$$

In the macroscopic limit

$$aq_0 \to \frac{D}{T} \left[\partial_x T|_{(-0)} - \partial_x T|_{(+0)} \right] \tag{53}$$

This implies that the source density q_0 is singular but the total source $Q_0 = aq_0$ inside cell 0 is finite.

It is worth comparing this with the thermodynamic treatment of this situation where there is a jump in the entropy current, in order to have finite entropy flux density Φ in each point, it is unavoidable to consider a $\tilde{\Phi}$ which is not a full divergence:

$$\Phi = -\partial_x j^{(s)} + \tilde{\Phi} \tag{54}$$

The form of $\tilde{\Phi}$ is obtained by integrating (54) around the point where the jump in the derivative appears ($x = 0$):

$$\int_{-\varepsilon}^{\varepsilon} \Phi\, dx = -j^{(s)}|_{(-\varepsilon)}^{(+\varepsilon)} + \int_{-\varepsilon}^{\varepsilon} \tilde{\Phi}\, dx \tag{55}$$

Smoothness of Φ requires that for $\varepsilon \to 0$

$$\int_{-\varepsilon}^{\varepsilon} \tilde{\Phi}\, dx = -j^{(s)}|_{(-0)}^{(+0)} \tag{56}$$

The multibaker result (46) implies that if q is singular as in cell 0, then $\Phi_0^{(th)} = \gamma \varrho q_0$. We then immediately see that $\Phi_0^{(th)}$ is the analog of $\tilde{\Phi}$. Indeed, by inserting the expression (47) for $j^{(s)}$ we have

$$\int_{-\varepsilon}^{\varepsilon} \tilde{\Phi}\, dx = \frac{\lambda}{T} \left[\partial_x T|_{(+0)} - \partial_x T|_{(-0)} \right] \tag{57}$$

which, on account of $\lambda = \gamma \varrho D$, exactly corresponds to (53).

We have shown, that the thermodynamic evaluation and the macroscopic limit of q_0 lead to the same result. Physically this means, that by a proper choice of the source terms even the singularity in the entropy flux can be described in full harmony with thermodynamics, and up to a factor of T the flux let into the thermostat is exactly the amount of heat that is taken out also in the thermodynamic description of a system with a bend in the temperature profile.

4. CROSS EFFECTS IN A MULTIBAKER MODEL

Thermodynamic cross effects, which probe the (off-diagonal) Onsager coefficients, are difficult to observe in homogeneous systems. When two materials are put into contact, however, they play a dominant role in understanding the heat and entropy currents. In order to mimic such phenomena, we consider two multibaker chains containing the cells $m=-M' \cdots -1$ and $m=0 \cdots M$, respectively, $(M, M' \gg 1)$ which are brought into contact at $m=0$ (cf. Fig. 6). Now, the parameters l^-, s^-, r^- and l^+, s^+, r^+ in the two parts are different, and for generality we will also assume that the constant reference densities $\varrho^{\star,\pm}$ are different. These differences will represent the different thermodynamic and transport properties of the materials. The difference in r and l gives rise to different drifts (conductivities) and diffusion coefficients, and the one in the reference density might be thought of reflecting for instance a different effective mass of the electrons.

As in the previous subsection, the dynamics of this multibaker chain drives a density and a kinetic-energy field. In order to simplify the structure of the steady-state density profiles, we restrict to the case $r^+/l^+ = r^-/l^-$. This choice is motivated by a physical interpretation of r/l. After all, the macroscopic limit of r/l is $1 + av/D$, and v/D is proportional to the external (electric) field, such that the requirement expresses that the external field

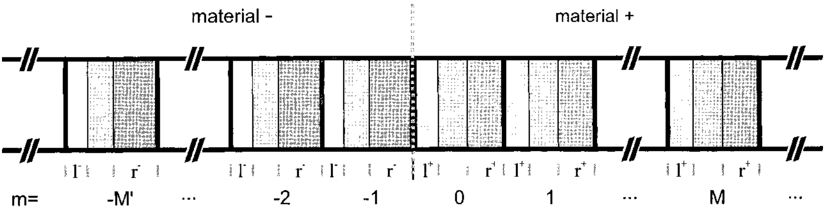

Fig. 6. Two long multibaker chains, representing materials $-$ and $+$, joined together at the junction between cells -1 and 0. The leads are in cells $-M'$ and M.

should be the same in both materials. In the remainder of this section we discuss the transport in this model in two different settings: (i) a constant (non-vanishing) particle current and constant temperature; (ii) vanishing particle current and an isolated system which is only thermostated at the "junction" $m=0$ and at the two "leads" $m=-M'$ and $m=M$, respectively. Setting (i) allows us to discuss the Peltier effect, and setting (ii) is used to describe the Seebeck effect.

Before turning to these specific settings, however, we discuss the steady state profile of the (particle) density in general. One does not expect noticeable gradients in the electron density in either material, so that we fix them to the constant values ϱ^- and ϱ^+, leading to the spatially uniform current [cf. (9)]

$$j=\frac{a}{\tau}(r^+-l^+)\,\varrho^+=\frac{a}{\tau}(r^--l^-)\,\varrho^-$$

In order to have the same current also across the junction, one has to require $l^-\varrho^-=l^+\varrho^+$ in addition. Together with the fact that v/D is fixed for the whole system, this implies that there is a constant amount of Joule's heating vj/D per unit length of the system, which either has to be transferred to a local thermostat [cf. (46)], or leads to a local heating, i.e., enforces non-uniform temperature profiles.

4.1. The Peltier Effect

The requirement of a constant temperature in the setting of the Peltier effect requires the use of a thermostated dynamics, $q=0$. In that case the Joule heating is transferred to the thermostat. Away from the junction, this leads to the flux $\Phi^{(th)}=vj/D$. In the entropy balance the difference in the materials shows up *only* in the entropy currents. In view of (47) and (48), they become different in the two parts of the multibaker

$$j^{(s,\,\pm)}=-j\left(1+\ln\left[\frac{\varrho^{\pm}}{\varrho^{\star\pm}}\,T^{-\gamma}\right]\right)=\frac{e\Pi^{\pm}}{T}\,j$$

implying that at the junction (i.e., between cells $m=-1$ and $m=0$) an additional heat flux, the *Peltier heat*, is directed to the thermostat. It is characterized by the difference of the entropy currents

$$j^{(s,\,+)}-j^{(s,\,-)}=-j\,\ln\frac{\varrho^+/\varrho^{\star+}}{\varrho^-/\varrho^{\star-}}=j\left[\ln\frac{l^+}{l^-}+\ln\frac{\varrho^{\star+}}{\varrho^{\star-}}\right]\equiv\frac{e\Pi^{(+/-)}}{T}\,j$$

where $\Pi^{(+/-)}$ defines the mutual Peltier coefficient of the two materials. It characterizes the amount of Peltier heat produced per unit electric current, ej, and is the difference of the material Peltier coefficients [cf. (48)]

$$\Pi^{(+/-)} = \Pi^{+} - \Pi^{-} \tag{58}$$

as also found in thermodynamics.

4.2. The Seebeck Effect

The Seebeck effect is observed in a thermally isolated system, where the junction is kept at a temperature T_j different from the temperature T_l prescribed at the leads, i.e., for the multibaker we demand $T_{-M'} = T_M = T_l$ and $T_{-1} = T_0 = T_j$. This setup corresponds to a non-uniform temperature field, and, due to this, also to gradients in the electro-chemical potential μ. Because of the difference in the material properties, these gradients can add up to a net potential drop between the leads, even if both leads are kept at the same temperature and there is no particle current. This follows immediately from the formal definition$^{(23)}$ of the particle current in its discrete version:

$$j_m \equiv -\frac{\sigma_{el}}{e^2}\left[\frac{\mu_{m+1}-\mu_m}{a} + e\alpha\,\frac{(T_{m+1}-T_m)}{a}\right] \tag{59}$$

where σ_{el} is the conductivity, e the electric charge, and α the Seebeck coefficient of the material. In the considered system, we then have for vanishing current

$$\begin{aligned}\mu_{-M'}-\mu_M &= \mu_{-M'}-\mu_{-1}+\mu_{-1}-\mu_0+\mu_0-\mu_M\\ &\approx -e\alpha^{-}(T_{-M'}-T_{-1})+\mu_{-1}-\mu_0-e\alpha^{+}(T_0-T_M)\\ &= e(\alpha^{+}-\alpha^{-})(T_l-T_j)+\mu_{-1}-\mu_0\end{aligned} \tag{60}$$

Here we have assumed the Seebeck coefficients to be approximately constant in the two materials. The macroscopic limit implies $\mu_{-1} = \mu_0$, and we obtain for the mutual Seebeck coefficient of the two materials$^{(29)}$

$$\alpha^{(+/-)} \equiv \frac{\mu_{-M'}-\mu_M}{e(T_l-T_j)} = \alpha^{+}-\alpha^{-} \tag{61}$$

It characterizes the strength of the potential drop $\mu_{-M'}-\mu_M$ between the leads induced by the temperature difference $T_l - T_j$ between the leads and the junction.

An expression for $\alpha^{(+/-)}$ can be determined for the multibaker by rewriting the expression (27) for the current in the form (59). Taking immediately the macroscopic limit and observing that the electro-chemical potential can be split into a chemical part μ_c and a part $e\phi$ due to the external electric field $E \equiv -\partial_x \phi$, one obtains

$$\begin{aligned} j &= -\frac{\sigma_{el}}{e^2} [\partial_x(\mu_c + e\phi) + e\alpha\, \partial_x T] \\ &= \frac{\sigma_{el} E}{e} - \frac{\sigma_{el}}{e^2} [\partial_\varrho \mu_c\, \partial_x \varrho + \partial_T \mu_c\, \partial_x T + e\alpha\, \partial_x T] = v\varrho - D\, \partial_x \varrho \end{aligned} \tag{62}$$

Here

$$v = \frac{\sigma_{el} E}{e\varrho} \tag{63a}$$

$$D = \frac{\sigma_{el}}{e^2} \partial_\varrho \mu_c \tag{63b}$$

$$e\alpha = -\partial_T \mu_c \tag{63c}$$

By the first two equations we recover well-known relations from thermodynamics.⁽²³⁾ Equation (63c) provides us with a relation for the Seebeck coefficient. Since the equation of state of the "multibaker gas" is that of a classical ideal gas⁽¹⁸⁾

$$\mu_c^{\pm} = (\gamma + 1)\, T + T \ln \left(\frac{\varrho^{\pm} T^{-\gamma}}{\varrho^{\star \pm}} \right)$$

one obtains

$$\begin{aligned} e\alpha^{(+/-)} &= e(\alpha^+ - \alpha^-) = e \ln \frac{\varrho^+ T_l^{-\gamma}}{\varrho^{\star +}} - e \ln \frac{\varrho^- T_l^{-\gamma}}{\varrho^{\star -}} \\ &= e \left[\ln \frac{l^+}{l^-} + \ln \frac{\varrho^{\star +}}{\varrho^*} \right] = \frac{e\Pi^{(+/-)}}{T_l} \end{aligned}$$

where (58) was used in the last step. This comparison expresses the validity of the Onsager relation $\Pi^{(+/-)} = \alpha^{(+/-)} T$ for this class of models.

5. DISCUSSION

In this paper we have described the local and global transport properties of multibakers with a density and energy dynamics. This class of maps makes an analytical modeling of transport processes by a deterministic chaotic dynamics possible, and admits a macroscopic description consistent with various aspects of irreversible thermodynamics. The macroscopic description comprises the time evolution of the average density and the kinetic energy in small regions of the physical space (the cells of the multibaker). The former density is interpreted as the particle density, and the latter as a temperature field. The averages in the small regions are in the spirit of local thermodynamic equilibrium, and the continuum description of thermodynamics arises in a macroscopic limit where the spatial resolution of the transport process is small compared to the system size (or any other relevant macroscopic length), and where a discrete time-scale used in the definition of the dynamics is much smaller than macroscopic time scales.

The relevant concept of entropy for multibakers is the Gibbs entropy defined with respect to the average density in the cells normalized by a temperature-dependent reference density. It is called the coarse-grained entropy. Based on an information-theoretic interpretation of the entropy, a local entropy balance can be derived, which in the macroscopic limit can be fully consistent with irreversible thermodynamics. This agreement holds provided that (i) a particular choice of local phase-space contraction and expansion rates is incorporated in the time evolution of the density, which we identified as a time-reversible evolution of the mapping in previous work,(12, 14, 15) (ii) the density in the entropy is normalized by a reference density with a power-law dependence on the average kinetic energy in the cell, and (iii) appropriate source terms are incorporated in the evolution equations of the kinetic-energy field. No meaningful macroscopic description can be found for multibakers with other choices of the phase-space contraction factors. Modification of the source terms leads to additional contributions in the local entropy balance, which are interpreted as local entropy fluxes into a thermostat. In particular, for vanishing source terms one can mimic a transport process in a system with a spatially uniform temperature, i.e., one obtains a setting reminiscent of NEMD simulations of transport processes.

Once the connection between the deterministic dynamics of the multibaker and the corresponding local thermodynamic relations is established, one can apply it to discuss transport in different macroscopic settings. A number of models with periodic boundary conditions were discussed in order to shed light on the global entropy balance in such systems. We find that, up to a trivial factor, the globally averaged phase-space contraction rate amounts to the entropy flux to the environment. In contrast to the claims of some authors (cf., for instance, ref. 28) the connection between the irreversible entropy production and the phase-space contraction rate breaks down away from stationarity. In fact, the contraction rate is still connected to the entropy flux in that situation, but the flux is no longer related to the rate of irreversible entropy production. This was shown (a) for multibakers with a uniform thermostatting (Model II), i.e., for models reminiscent of NEMD algorithms, and (b) for systems where the driving and thermostating is applied in a macroscopically small region of the system (Model III), thus giving rise to sustained density gradients. In systems with a uniform external field and localized thermostating (Model IV) the total entropy flux contains the integral of the local heating factors besides the phase-space contraction rate. The former two models have constant temperature fields, while the latter one supports a temperature profile with a discontinuity in the first derivative at the position of thermostating. As expected from the existence of the local entropy balance, the results are fully consistent with the corresponding thermodynamic description of the transport process. They suggest an interesting conclusion on modeling transport in bulk systems by isothermal NEMD simulations: These methods are valid in an approximation where the considered volume is sufficiently small to neglect density and temperature gradients. In steady states, they are equivalent to models, where the currents are the same, but thermostating is only applied at the boundaries of a macroscopic system. Since even state-of-the-art simulations can hardly cope with more than 10^9 particles, i.e., with integration volumes larger than about one $\mu\mathrm{m}^3$, this approximation seems to be well-justified in numerical studies. On the other hand, this assumptions should be kept in mind when isothermal NEMD modeling is taken as basis of theoretical studies of transport processes (cf., for instance, refs. 3–5, 27).

To further demonstrate the use of multibakers with density and energy fields, we also discussed thermoelectric cross effects. The description of the transport properties requires in that case information on the equation of state, since the Seebeck effect is defined in terms of differences of chemical potentials. In previous work(17, 18) it was shown that the classical ideal-gas equation holds for multibakers. This is meaningful since the time evolution of the multibaker can be considered as the one of particles with phase-space coordinates (x, p), which only interact by a (weak) mean-field like coupling manifested in a dependence of the local parameters on the average densities. With this input the Peltier and Seebeck effect were modeled and the Onsager relation, connecting their respective transport coefficients, was derived. The validity of this relation for multibakers is not a trivial result. It heavily relies on the choices (i)–(iii) to find an entropy balance consistent with irreversible thermodynamics.

Summarizing, we demonstrated that multibakers establish a straightforward modeling of various transport phenomena by a deterministic, chaotic dynamics. They give insight in the general structure of such models by explicit analytical calculations. This was demonstrated by discussions of thermoelectric cross effects, and of the relation between the average phase-space contraction, entropy fluxes and the rate of irreversible entropy production.

ACKNOWLEDGMENTS

This work is dedicated to Prof. Gregoire Nicolis on the occasion of his 60th birthday. Our discussions at the *Centre of Complex Systems and Nonlinear Phenomena* helped us a lot, when we were starting this project in the summer of 1998. We are also grateful to J.R. Dorfman, B. Fogarassy, J. Hajdu, G. Tichy, and H. Posch for enlightening discussions. The paper was completed during a joint stay at the *Max Planck Institute for the Physics of Complex Systems*, which we gratefully acknowledge together with a support from the Hungarian Science Foundation (OTKA T17493, T19483) and the TMR-network *Spatially extended dynamics.*

REFERENCES

1. D. J. Evans and G. P. Morriss, *Statistical Mechanics of Nonequilibrium Liquids* (Academic Press, London, 1990); W. G. Hoover, *Computational Statistical Mechanics* (Elsevier, Amsterdam, 1991).
2. W. N. Vance, *Phys. Rev. Lett.* **69**:1356 (1992).
3. N. I. Chernov, G. L. Eyink, J. L. Lebowitz, and Ya. G. Sinai, *Phys. Rev. Lett.* **70**:2209 (1993); *Comm. Math. Phys.* **154**:569 (1993).
4. D. J. Evans, E. G. D. Cohen, and G. P. Morriss, *Phys. Rev. Lett.* **71**:2401 (1993).
5. G. Gallavotti and E. G. D. Cohen, *Phys. Rev. Lett.* **74**:2694 (1995); *J. Stat. Phys.* **80**:931 (1995).
6. K. Rateitschak, R. Klages, and G. Nicolis, *J. Stat. Phys.* **99**:1364 (2000).
7. J. R. Dorfman, *An Introduction to Chaos in Non-Equilibrium Statistical Mechanics* (Cambridge University Press, Cambridge, 1999); *Chaos* **8**:2 (1998), Focus issue on *Chaos and Irreversibility*.
8. N. I. Chernov and J. L. Lebowitz, *Phys. Rev. Lett.* **75**:2831 (1995); *J. Stat. Phys.* **86**:953 (1997); Ch. Dellago and H. A. Posch, *J. Stat. Phys.* **88**:825 (1997).
9. C. Wagner, R. Klages, and G. Nicolis, *Phys. Rev. E* **60**:1401 (1999).
10. P. Gaspard, *J. Stat. Phys.* **68**:673 (1992).
11. S. Tasaki and P. Gaspard, *J. Stat. Phys.* **81**:935 (1995).
12. J. Vollmer, T. Tél, and W. Breymann, *Phys. Rev. Lett.* **79**:2759 (1997).
13. P. Gaspard, *Physica A* **240**:54 (1997); *J. Stat. Phys.* **88**:1215 (1997).
14. J. Vollmer, T. Tél, and W. Breymann, *Phys. Rev. E* **58**:1672 (1998).
15. W. Breymann, T. Tél, and J. Vollmer, *Chaos* **8**:396 (1998).
16. T. Gilbert, C. D. Ferguson, and J. R. Dorfman, *Phys. Rev. E* **59**:364 (1999); T. Gilbert and J. R. Dorfman, *J. Stat. Phys.* **96**:225 (1999).

17. L. Mátyás, T. Tél, and J. Vollmer, *Phys. Rev. E* **61**:R3295 (2000).
18. L. Mátyás, T. Tél, and J. Vollmer, *Phys. Rev. E* **62**:349 (2000).
19. S. Tasaki and P. Gaspard, *Theoretical Chemistry Accounts* **102**:385–396 (1999); *Entropy Production and Transports in a Conservative Multibaker Map with Energy*, this volume.
20. P. Gaspard, *Scattering*, *Chaos and Statistical Mechanics* (Cambridge University Press, Cambridge, 1998).
21. G. Nicolis and D. Daems, *J. Phys. Chem.* **100**:19187 (1996).
22. D. Daems and G. Nicolis, *Phys. Rev. E* **59**:4000 (1999).
23. S. R. de Groot and P. Mazur, *Nonequilibrium Thermodynamics* (Elsevier, Amsterdam, 1962) (reprinted: Dover, New York, 1984).
24. D. Ruelle, *J. Stat. Phys.* **85**:1 (1996); **86**:935 (1997).
25. W. Breymann, T. Tél, and J. Vollmer, *Phys. Rev. Lett.* **77**:2945 (1996).
26. L. Rondoni and G. P. Morriss, *Phys. Rev. E* **53**:2143 (1996).
27. G. Gallavotti, *Phys. Rev. Lett.* **77**:4334 (1996); *J. Stat. Phys.* **86**:907 (1997).
28. L. Rondoni and E. G. D. Cohen, *Nonlinearity* **13**:1905 (2000).
29. N. W. Ashcroft and N. D. Mermin, *Solid State Physics*, Chap. 16 (Holt, Reinehart and Winston, Saunders College, Philadelphia, 1976).